An automated system for detecting ocular diseases with computer-aided tools is essential to identify different eye disorders through fundus pictures. This is because diagnosing ocular illnesses manually is a complicated, time-consuming, and error-prone process. In this research, two multi-label embedded architectures based on a deep learning strategy were proposed for ocular disease recognition and classification. The ODIR (Ocular Disease Intelligent Recognition) dataset was adopted for those models. The suggested designs were implemented as parallel systems. The first model was developed as a parallel embedded system that leverages transfer learning to implement its classifiers. The implementation of these classifiers utilized the deep learning network from VGG16, while the second model was introduced with a parallel architecture, and its classifiers were implemented based on newly proposed deep learning networks. These networks were notable for their small size, limited layers, speedy response, and accurate performance. Therefore, the new proposed design has several benefits, like a small classification network size (20 % of VGG16), enhanced speed, and reduced energy consumption, as well as the suitability for IoT applications that support smart systems like Raspberry Pi and Self-powered components, which possess the ability to function as long as a charged battery is available. The highest accuracy of 0.9974 and 0.96 has been obtained in both proposed models for Myopia ocular disease detection and classification. Compared to research that had been presented in the same field, the performance accuracy of each of the two models shown was high. The P3448-0000 Jetson Nano Developer Kit is used to implement both of the proposed embedded models

Keywords: ocular diseases, fundus imaging, optical coherence tomography, deep learning, multi-label embedded architectures, parallel architecture, transfer learning, ODIR, training, validation

UDC 004
DOI: 10.15587/1729-4061.2023.281790

DCNN-BASED EMBEDDED MODELS FOR PARALLEL DIAGNOSIS OF OCULAR DISEASES

Mamoon A Al Jbaar
Corresponding author
Master of Science in Computer Engineering,
Assistant Lecturer
Department of Computer and Information Engineering
College of Electronics Engineering
Ninevah University
Al-Jusaq str., Cornish, Mosul, Iraq, 41001
E-mail: mamoon.thanoon@uoninevah.edu.iq
Shefa A. Dawwd
Professor of Computer Engineering PhD
Department of Computer Engineering
University of Mosul
Al Majmoaa str., Mosul, Iraq, 41001

Received date 28.04.2023
Accepted date 07.07.2023
Published date 30.08.2023

***How to Cite**: Al Jbaar, M. A., Dawwd, S. A. (2023). DCNN-based embedded models for parallel diagnosis of ocular diseases. Eastern-European Journal of Enterprise Technologies, 4 (2 (124)), 53–69. doi: https://doi.org/10.15587/1729-4061.2023.281790*

1. Introduction

An increasing number of people around the world are affected by eye diseases [1]. More importantly, some eye diseases cause irreversible blindness that cannot be cured, while some other diseases such as cataracts, glaucoma, high eye pressure, bulging vision, etc. lead to visual impairment [2]. In clinical settings, early detection of these diseases helps prevent visual damage. Despite this, there is still a huge gap between the number of ophthalmologists and the number of patients. Moreover, manual evaluation of the fundus takes time and relies heavily on ophthalmologists' skills, which makes intensive fundus examination more difficult. As a result, computer-aided diagnostic procedures to identify robotic eye problems are critical [3]. Ocular problems might manifest differently in various populations in both developed and underdeveloped nations [4]. Developing countries, particularly those in Asia, frequently have high rates of untreated and undertreated eye illnesses [5]. According to the World Health Organization, there will be a dramatic rise in the number of visually impaired people [6]; nearly two-thirds of these injuries are vision impairment caused by a combination of factors, the most common of which are uncorrected refraction, cataracts, age-related macular degeneration, glaucoma, diabetic retinopathy, corneal opacity, trachoma, high blood pressure, etc. [5]. Research in this area has shown that early identification and diagnosis can reduce the incidence of injuries by as much as half [7]. According to the Urban Health Survey conducted in 2013 [8], many low-income people who live in slums are generally in poor health. Due to these factors, it is crucial that these people have access to affordable or free medical care, especially preventative and emergency treatments in the field of optometry. However then, deep learning-based algorithms have taken center stage in the growing area of medical image analysis [9].

This is particularly so given that deep learning models have been shown to be effective in a wide range of applications, one of the most important is the classification of medical data and illness diagnosis [10]. To lessen the burden on an ophthalmologist, automated disease detection is essential [11]. While human intervention isn't always necessary, illnesses can be spotted by computerized methods like deep learning and computer vision. While several of these studies have shown promising results, only a select few have provided a complete diagnosis of numerous ocular disorders [12]. Most studies on identifying and diagnosing eye conditions have used deep learning networks that make use of transfer learning. Deep learning networks, on the other hand, have been used in some studies that adhere to the single-network principle, concentrating on a single input and making a single disease diagnosis at a time. In fact, it is urgent to develop deep learning network architectures and produce new architecture models relying on simple, modified deep learning networks that are suitable for standalone or remote artificial intelligence applications. In the majority of the studies done in this field, this aspect has not been fully explored [13]. This paper's research focuses on two main aspects aimed at creating an embedded system that can identify and diagnose multiple types of eye diseases concurrently. The principle of parallelism

in diagnosis is utilized in both approaches and various types of deep learning networks invested in both architectures. The two architecture models are both implemented using parallel approaches, which involve executing a single prediction command on multiple data sets simultaneously. The integration of parallel architectures into the development of deep learning systems has provided several benefits, rendering them superior to previous systems. These advantages include enhanced performance speed and increased flexibility in handling inputs. Additionally, deep learning systems can be deployed as independent embedded systems, providing the added benefit of mobility. Both proposed architectures have been implemented on the P3448-0000 model of the Jetson Nano Developer Kit. This paper utilized the ODIR dataset, which is the Ocular Disease Intelligent Identification database. This database is a well-organized collection of information on 5,000 patients, which includes demographic information such as age, fundus photographs of both eyes (10,000 images), and diagnostic keywords from ophthalmologists. The dataset was gathered by Shanggong Medical Technology Co., Ltd. to simulate a realistic sample of patient records from various medical facilities in China. The fundus photos in these facilities were captured using a range of cameras, including Canon, Zeiss, and Kowa, each of which produces slightly different picture quality [14]. The dataset used in this study was severely skewed, making it unsuitable for categorizing any disorders. This mismatch created considerable oscillations throughout training, which was troublesome. A balancing strategy was used to overcome this problem. In addition, instead of categorizing all diseases using the complete dataset, two classes were chosen for each disease: normal and eye disease x, where x is one of the eye disorders that the suggested design detects, where the classification process is accomplished simultaneously.

Researchers were motivated by the remarkable achievements of deep learning networks in detecting and diagnosing eye diseases. This has prompted them to delve further into enhancing the effectiveness and capabilities of these networks, striving to create highly accurate systems. The urgency arises from the escalating prevalence of these diseases, surpassing the capacity of medical resources. Consequently, there is a pressing need for expanded support to cater to the growing number of cases.

Therefore, studies that are devoted to developing deep learning models for ocular disease diagnosis are of scientific relevance.

2. Literature review and problem statement

There have been numerous endeavors aimed at precisely categorizing ocular disorders. Some of these efforts have focused on using fundus images to develop diagnostic systems, while others have utilized Optical Coherence Tomography (OCT) for the same purpose. So in [15], a pipeline classifier based on transfer learning is recommended as a method to automatically classify the severity of Cataracts. The authors show that a combined model of AlexNet, InceptionV3, Xception, and InceptionResNetV2 with a weighted average algorithm can distinguish between a normal cataract and a cataract with 99.20 % accuracy and between a normal cataract and a severe cataract with 97.76 % accuracy, and that is better compared with the independent models. The ensemble model also reduces the number of wrong classifications by an average of 2.17 %. One of the drawbacks of this study is that the proposed deep learning model focused solely on detecting and diagnosing one eye disease, without considering other potential ailments the patient might have.

Furthermore, the researchers introduced an intricate intelligent system comprising four complex deep learning networks. The implementation and training of these networks aimed to achieve high accuracy. However, a thorough analysis of the network's performance could have revealed the possibility of using a less complex deep network while still obtaining similar accuracy levels as demonstrated in our research.

A new deep learning model for Glaucoma detection was demonstrated in [16], relying on three openly accessible datasets: HRF, Origa, and Drishti GS1. The proposed architecture employed an Alexnet model trained with an SVM classifier and achieved a 91.21 % accuracy rate in correctly classifying images. Despite the researchers' integration of both machine learning and deep learning approaches to enhance the outcome, the accuracy attained is considerably lower in comparison to using a network such as Alexnet. Further, the research required some preprocessing of the input images, which could potentially enhance the results.

The study in [17] employed pre-transformed learning models in combination with the U-Net architecture, based on the principles of deep learning, to identify the presence of glaucoma in an individual. The model utilized a DenseNet-201 deep convolutional neural network (DCNN) and achieved a 96.90 % accuracy rate during testing. The study utilized the sequential model approach, where the classification aspect was based on DenseNet-201 and dependent on the initial portion designed by the U-Net architecture. However, a more effective implementation of this research could have been achieved by adopting a parallelism principle, whereby normal cases are isolated independently without relying on the classification of pathological cases. This would have resulted in an increase in the efficiency and speed of the model presented.

While in [18], ResNet-152, a deep learning model with an enhanced activation function, has been proposed for the detection of diabetic retinopathy (DR). To train and validate the model, DIARETDB0, DRIVE, CHASE, and Kaggle were used. On the Kaggle dataset, the model showed an excellent accuracy of 99.41 %, suggesting its potential as a useful tool for DR diagnosis. One obstacle of the proposed system is the utilization of a large deep learning network, such as ResNet-152 of size 58.157 M, only for the detection of diabetic retinopathy. This choice overlooks the association of this disease with other eye conditions like glaucoma and elevated eye pressure.

Additionally, there is no analysis for the ResNet-152 model to simplify it and decrease its complexity via dropping out or truncating the ineffective layers. Instead, the system utilizes the conventional sequential form of ResNet-152, resulting in increased resource consumption, including memory and other storage capacities.

An automated approach for detecting Ocular Hypertension (OHT) using a deep learning model is presented in [19]. The model is built using ResNet-50 and trained on a dataset of 66,715 images. The proposed method has demonstrated high efficacy in diagnosing OHT, achieving a success rate of 95 %. The study has identified multiple weaknesses that necese sitate attention, specifically the lack of consideration given to the balance between normal and infected cases in the database utilized for model training. This lack of consideration resulted in biased and unfair decisions being made. Additionally, the database was not pre-processed, despite containing numerous poor-quality images, leading to possible misclassification. Moreover, the issue of image scaling proved to be problematic

as it led to the loss of crucial information, ultimately affecting the training outcomes of the suggested model. It was possible to take into account these points with the adoption of a less complex deep learning network and obtain better results.

In addition, a new classification algorithm based on Glaucoma Net is presented in [20] to automatically detect Primary Open-Angle Glaucoma (POAG) cases. The algorithm achieves high accuracy for both the Ocular Hypertension Treatment Study (OHTS) participants and the Large-scale Attention-based Glaucoma (LAG) dataset. The proposed design has a lower sensitivity compared to other related articles, as well as the imbalance in the dataset used for its training, the model. This makes its decision unfair.

In [21], the authors investigate the potential of deep learning (DL) algorithms for the automated classification of Macular Diseases on OCT images, using a two-step DL algorithm. The study employs RelayNet for automated segmentation of the OCT images before classification, yielding sensitivity, specificity, and accuracy of 72.90 %, 96.20 %, and 93.92 %, respectively. However, a major drawback of the study is the use of the six-line scan, which results in bias and may lead to mislabeling some OCT scans as diseased when they appear normal. Additionally, the algorithm's sensitivity is low. Furthermore, the DL models' applicability to OCT images from other devices remains unknown as the study relied solely on a specific brand of OCT device.

The authors suggested a transfer learning model based on deep learning in [22] to automatically diagnose Dry Eye (DE) by classifying individual video frames, the dataset comprised 128 eyes of 128 patients with DE and 116 eyes of 116 healthy subjects. They tried three different deep learning networks in their design, DenseNet121, ResNet50V2, and Inception V3. The best results have been obtained via ResNet50V2, which are 0.9, 0.84, 0.99, 0.91 for accuracy, recall, precision, and F1 score. The drawbacks of this study can be briefly the large numbers of the frame and augmented images and the high similarity of the extracted frame of the same video. Besides that, the proposed model was ungeneralized because of its reliance on the selected dataset. Also, the model suffers from overfitting in its CNN.

A deep learning classification model based on transfer learning using VGG19 has been employed in [23]. Utilizing Optical Coherence Tomography (OCT) technique, the model has been trained to classify optical coherence tomography (OCT) scans into one of four conditions that affect the retina, including choroidal neovascularization, drusen, diabetic macular edema, and normal. The results indicate that this proposed model has achieved outstanding performance, with a remarkable classification accuracy of 99.17 %. The researchers emphasize the impressive level of accuracy attained by their proposed system. However, they pointed out that this accuracy is influenced by the settings of the devices and the methodology employed for capturing retinal images. They point up that the performance of their system is entirely dependent on these factors.

Furthermore, another factor that restricts the performance of the system presented in this study is the requirement for a substantial volume of data for training and testing purposes. It is highlighted that the achieved accuracy is contingent upon the availability of a significant amount of data. Conversely, if only a limited amount of data is available, the system fails to achieve a similar level of accuracy or even a close approximation.

A deep learning model was developed in [24] to diagnose pathological myopia automatically. Their proposed method involved transfer learning from four pre-trained convolutional neural networks: ResNet18, ResNet50, EfficientNet B0, and EfficientNet B4. The model was trained on a dataset of 367 3D optical coherence tomography images, and the evaluation of the four networks showed that the EfficientNetB4 model had the highest accuracy of 95 %. Hence, the EfficientNetB4 model is a suitable choice for diagnosing pathological myopia. Nonetheless, the project exhibits certain limitations. The study involved a sample size of 37 eyes, out of which 13 eyes with pathologic myopia were evaluated for performance using OCT. Furthermore, it is noteworthy that merely the en-face OCT image generated in the anterior segment of the retinal layer was utilized. It is worth mentioning that the majority of deep learning models that employ OCT data typically utilize B-scan, thereby providing a unique viewpoint. Furthermore, it should be noted that the study was conducted with only patient data from Korea. As a result, the efficacy of the proposed system may vary when tested on a database comprising individuals from diverse ethnic backgrounds. The prevalence of pathologic myopia varies among different races.

Upon reviewing a collection of works pertaining to the diagnosis and classification of eye diseases and conducting an analysis of their proposed systems and achieved results, it became evident that there remain significant areas yet to be processed, and overcoming numerous identified obstacles. Firstly, most studies commonly employ deep learning networks that follow the principle of a single consecutive network. However, this approach introduces considerable complexity to the computational operations within the neural network. As a result, it becomes challenging to train and implement such networks, impacting their accuracy and operational flexibility.

Secondly, a recurring issue observed in most studies is the problem of database imbalance, which results in a lack of impartiality and accuracy in diagnostic decisions, as well as most of these studies did not utilize pre-processing of data images, which could improve performance and resolution correction within the system.

Furthermore, no innovation of any deep learning network was presented with low complexity, easy training and implementation, and suitability for remote and self-powered applications, as most studies relied on well-known deep learning networks.

All this allows us to assert that it is expedient to conduct a study to present systems that address all the above points through new and innovative deep learning networks based on parallel architectures in low-cost embedded systems.

3. The aim and objectives of the study

The aim of the study is to diagnose and classify various ocular diseases simultaneously using a low-cost, energy-efficient multiclass classification system, with newly presented architectures models, that achieve high accuracy, low computation complexity, and fast response.

To accomplish the aim, the following objectives have been set:

– to present a developed design and implementation of embedded models that are able to detect and classify eight ocular diseases concurrently via employing parallel architecture approaches throughout the development of the proposed systems;

– to employ new proposed deep networks for implementing those designs to increase the efficiency of the system and

provide the system with the capability to simultaneously diagnose and classify more than one eye disease for each entry.

4. Materials and methods

The object of the study is to develop independent and mobile embedded systems for the detection and classification of eye diseases.

The main hypothesis in the context of our study is to propose new deep learning networks and investment of parallel architectures as the basis for the implementation of the proposed models to achieve high accuracy, superior performance speed, and obtain concurrent results, as well as reduce the complexity of calculations within the neural network.

The ODIR dataset was used to train both presented models, which are implemented on a parallelism support platform, Jetson Nano.

ODIR is a database of structured ophthalmic data comprising 5,000 patients of both eyes. It includes information such as age, color fundus photographs from both left and right eyes, and diagnostic keywords provided by doctors. This dataset is intended to reflect real-world patient information collected by Shanggong Medical Technology Co., Ltd. from multiple hospitals and medical centers throughout China. The fundus images in this database were captured using different cameras available in the market, including Canon, Zeiss, and Kowa, resulting in varying image resolutions. This data set presents a variety of challenges. To begin with, the overwhelming number of photographs is poorly lit and unclear, necessitating preprocessing before they can be used as inputs in the proposed system. So, histogram equalization was employed as a simplified image processing technique to enhance the quality of images that are used for training and testing of the deep learning networks. Furthermore, the dataset for particular ocular ailments exhibits significant class imbalance [25], as shown in Fig. 1. So, as a result of this significant imbalance within the datasets, the accuracy of both disease and normal image detection and classification is relatively low. Hence, attempting to classify any disease using this dataset is inadvisable, as it results in significant fluctuation during training. To address this issue, one of the possible solutions suggested in this study is to balance the images between the two classes. Besides that, instead of processing all images and classifying all diseases at once, the suggested approach takes two classes at a time and balances them by taking the same number of images from both classes and feeding them into a pre-trained deep network. This dataset was divided into an 80:20 ratio, with 80 % of the data being used for training and 20 % for testing purposes.

The ocular diseases detected and classified in this paper research are Cataracts (C), moderate non-proliferative diabetic retinopathy (D), Myopia (M), Ocular hypertension (H), Glaucoma (G), dry age-related macular degeneration (A), and Others (O). Besides, the Normal case that represents a health condition that does not suffer from the above diseases Fig. 2 clarifies the fundus image for each of those diseases.

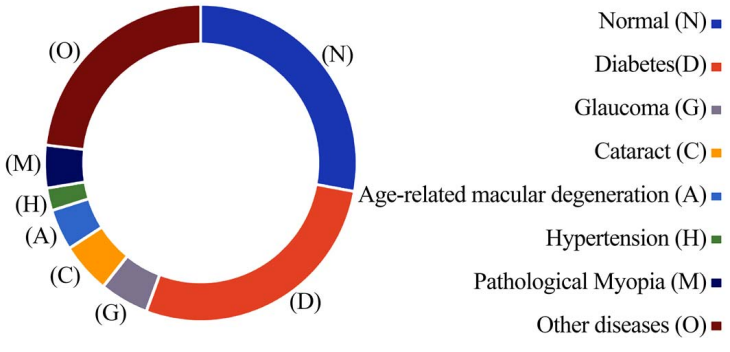

Fig. 1. Ocular diseases in ODIR dataset image distribution

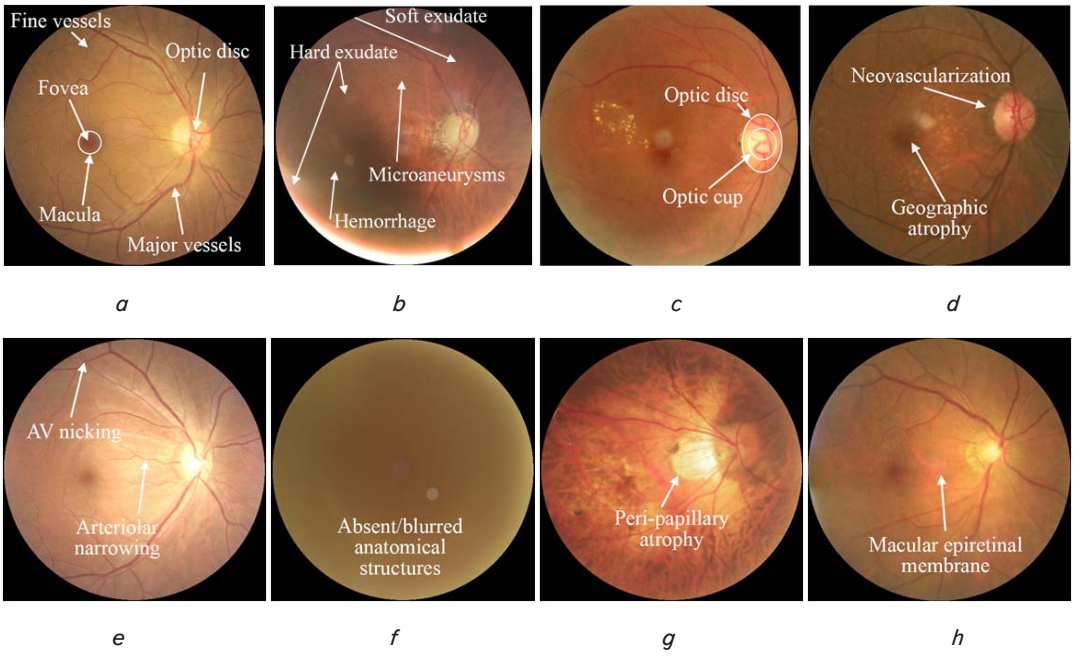

Fig. 2. Fundus images from the ODIR dataset showing anatomical structures and abnormalities due to various ophthalmological diseases: *a* – normal image; *b* – glaucoma; *c* – diabetic retinopathy: *d* – AMD; *e* – hypertension; *f* – cataract; *g* – myopia; *h* – other abnormalities

So for those diseases, we can give a brief overview that includes the causes, symptoms, and warning signs of each of these conditions will be examined:

1. Cataracts (C).

The formation of protein aggregates on the eye's lens leads to the development of cataracts, which manifest as a hazy, thick mass. This mass obstructs the normal passage of light to the retina, resulting in reduced night vision, fuzzy vision, dulled colors, and double vision [26]. Major risk factors for cataract development include smoking, being overweight, having high blood pressure, having a family history of cataracts, having diabetes, and being exposed to radiation from X-rays or cancer treatments. Cataracts are one of the most common eye ailments and are particularly prevalent in poor and middle-income countries [27].

2. Moderate non-proliferative diabetic retinopathy (D).

Non-proliferative diabetic retinopathy is an eye-related complication that can occur in people with diabetes. Non-proliferative diabetic retinopathy is the initial stage of this condition and can be effectively managed with prompt identification and treatment. Over half of individuals with diabetes will eventually develop diabetic retinopathy, and the likelihood increases with the duration of the disease. The retina, a light-sensitive tissue located at the back of the eye, contains blood vessels that can be damaged over time due to high blood sugar levels. Early diabetic retinopathy causes these blood vessels to weaken and form microaneurysms, leading to fluid leakage and swelling in the retina's center, known as the macula. Blood vessel closure can also result in macular ischemia. If left untreated, non-proliferative diabetic retinopathy can progress to a more severe form in which fragile new blood vessels develop in the retina. These vessels can leak blood and fluid into the vitreous gel at the back of the eye, causing further damage and vision loss. Therefore, early detection and treatment of diabetic retinopathy are crucial to prevent additional harm to the eyes [28].

3. Myopia (M).

The highest prevalence rates of myopia, the most prevalent ocular condition in young children, are found in East Asian countries. When myopia is severe and causes excessive axial elongation of the eye, it can stretch the outer coats of the eyeball, leading to various pathologic changes such as staphyloma, chorio-retinal atrophic lesions, lacquer cracks, and choroidal neovascularization. The "META analysis for Pathologic Myopia (META-PM)" study group has categorized myopic maculopathy signs into five categories: Category 0 for eyes with no macular lesions, Category 1 for those with a tessellated fundus, Category 2 for those with diffuse chorio-retinal atrophy, Category 3 for those with patchy chorio-retinal atrophy, and Category 4 for those with macular atrophy. An eye is considered to have pathologic myopia only when the fundus photography signs are consistent with category 2 and above [29].

4. Ocular hypertension (H).

When the drainage of fluid inside the eye, called aqueous humor, is inadequate, it leads to a condition known as ocular hypertension (H). People who are over the age of 40 or have a family history of ocular hypertension, glaucoma, or diabetes are at a higher risk of developing H. Uncontrolled high blood pressure or diabetes can also increase the vulnerability of patients to ocular hypertension. Those who have these risk factors should undergo regular eye check-ups to keep an eye on their ocular health and identify any possible problems at an early stage [30].

5. Glaucoma (G).

Glaucoma, a group of disorders that affect the eyes, can lead to progressive optic neuropathy and vision loss due to degeneration of the optic nerves. The cells of the optic nerve play a crucial role in transforming optical impulses into electrical impulses that the brain requires for visual processing. The primary causes of glaucoma include elevated intraocular pressure caused by aqueous fluid, genetic predisposition, and diabetes. Regardless of the level of intraocular pressure (high, normal, or low), glaucoma can cause damage that results in a loss of peripheral vision [31]. Certain types of glaucoma may have a sudden onset, and early diagnosis is crucial for preserving eyesight. One significant change in glaucoma is the increased ratio of cup area to disc area. Diagnosis of glaucoma involves measuring this ratio using color fundus pictures, analyzing visual fields with perimetry, and measuring intraocular pressure with a tonometer. Reference [32] discussed various glaucoma detection systems, with a particular emphasis on their suitability for mobile applications.

6. Dry age-related macular degeneration (A).

The incidence of age-related macular degeneration (AMD), a condition that primarily affects older adults, is on the rise as the population ages. In the initial stages of AMD, patients usually do not face any significant vision issues. However, without prompt intervention, central vision may be diminished or entirely lost. Consequently, early detection plays a crucial role in preventing the future advancement of AMD [33, 34].

7. Others (O).

The ODIR dataset comprises over eight distinct ocular diseases, while the remaining eye conditions were categorized as "other abnormal conditions".

This study presented an integrated system designed with parallel architectures to diagnose and classify multiple eye diseases simultaneously.

So, the first proposed model in this paper, which is Multi-label parallel embedded architecture transfer learning-based model, was implemented based on parallel architecture, where eight binary classifiers work in parallel, providing eight detecting and classifying operations at the same time. VGG 16 deep learning networks were adopted to construct the binary classifiers of the proposed model. The incorporation of parallelism in the presented systems architecture yields an independent and isolated diagnosis of each eye disease. Moreover, opting for parallelism in the implementation of deep learning networks, as opposed to relying on a single network principle, brought about several benefits, including faster disease diagnosis within a standard time. In addition, making the disease detection and classification process binary. This, in turn, reduced the operations within a single deep network, thereby decreasing the capacity consumed by a single neural network and minimizing the memory spaces reserved for the extracted image features.

Furthermore, the implementation of parallelism and independence approach for disease detection and classification has enabled the development of a diagnostic system that can identify multiple diseases simultaneously across various entries. Additionally, this approach allows for the detection and diagnosis of several diseases within a single entry, where eight ocular diseases can be detected and classified for one entry at the same time, as well as the possibility of the detection and classification of eight different diseases for eight entries concurrently. These advantages made it possible to implement the presented architecture as a standalone em-

bedded system that can operate independently. Fig. 3 gives a schematic description showing the parts of the proposed model. The process involves either broadcasting a single fundus image to seven binary classifiers, which work concurrently to detect and classify seven eye diseases, or inputting seven fundus images into the embedded system to detect and classify one ocular disease for each image.

As shown in Fig. 3, each binary classifier comprises a deep learning network, which is VGG16. For binary classification, two extra layers (flatten and dense of 1) were added to those networks to make the deep network to be binary classifier with two labels, Normal and specified ocular diseases.

Fig. 4 presents a comprehensive overview of the intricate particulars concerning the VGG16 network, which was adopted as a classifier in the first proposed model. These particulars include details such as the layer count, dimensions, activation function types, network parameters, and other related aspects.

The VGG16 network is constrained by a total of 14,714,688 parameters, as illustrated in Fig. 4, *b*. Moreover, two additional layers have been included as a modification to get a binary classifier. Unlike the sequential multi-class deep networks in our model, complex computations are fractured into eight parallel independent computation groups, which can be accomplished concurrently.

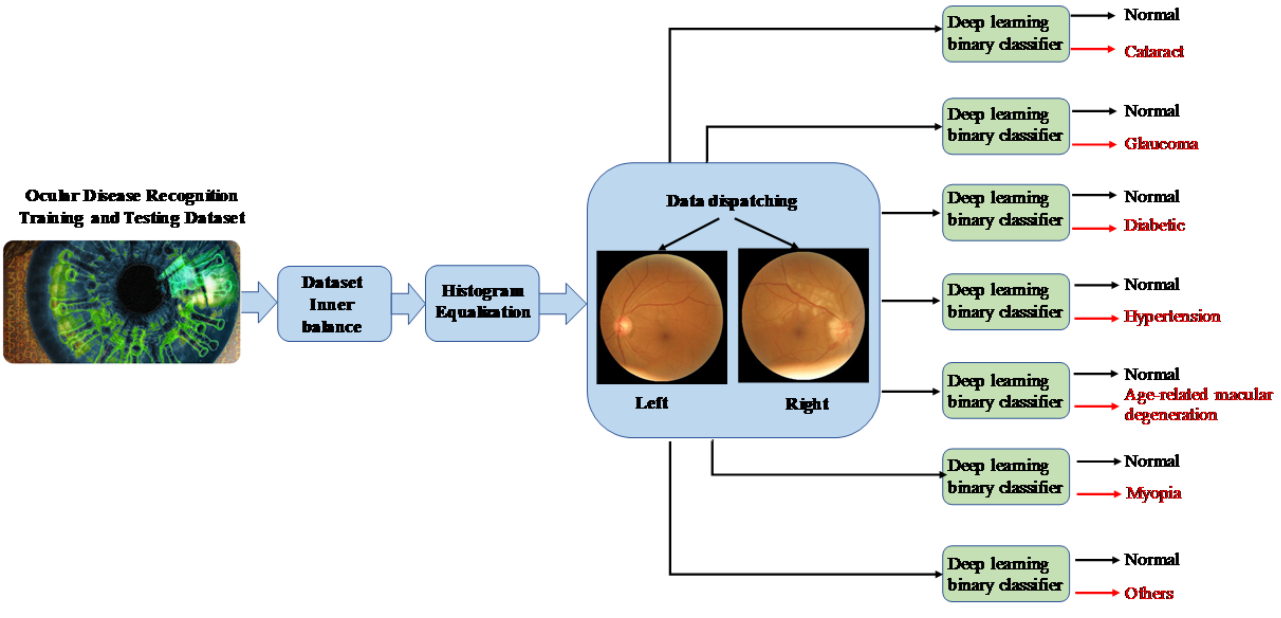

Fig. 3. Multi-label parallel embedded proposed model's architecture

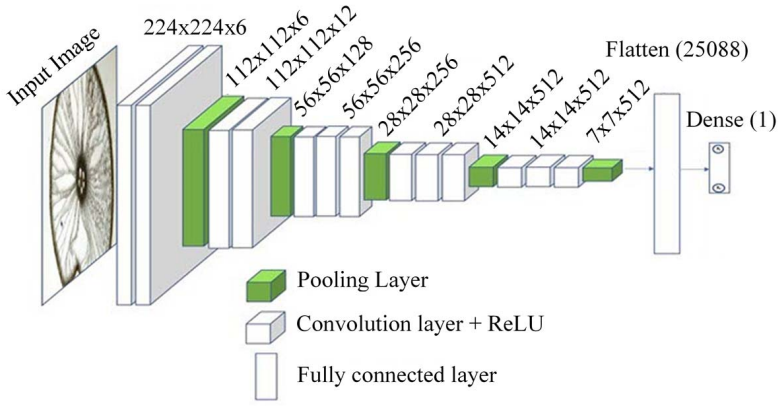

a

Model: "sequential_3"		
Layer (type)	Output shape	Param#
Flatten_3 (Flatten)	(None, 7, 7, 512)	14714688
Dense_3 (Dense)	(None, 25088)	0
Total params: 14,739,777	(None, 1)	25089
Trainable params: 14,739,777		
Non-trainable params: 0		

The added layers for binary classification

b

Fig. 4. Classifier layers details of the first proposed model: *a* – modified VGG16 deep network based on transfer learning; *b* – variables summary of the innovator learning network

In the second proposed model, which is Multi-label parallel embedded architecture novel deep network-based model, the same methodology of the parallel architecture was employed as in the first proposed model. The key feature that sets this model apart is its classifiers, which rely on novel deep learning networks that were presented, developed, and trained specifically for this model. The proposed approach involves constructing and optimizing deep learning networks that are well-suited for this model. As shown in Fig. 5, *a*. These networks exhibit exceptional performance and were developed following a thorough examination of the VGG16 network. This analysis involved tracking the extracted features at each layer, investigating and analyzing the impact of each layer on the network's resolution accuracy for all eight diagnosed and classified diseases. As a result, highly efficient networks were constructed, surpassing others in terms of their compact size and layer count within the field of deep learning.

Also, Fig. 5, *b* clarifies the deep network details, like the size of convolutional layers, pooling layers, as well as the network variable summary.

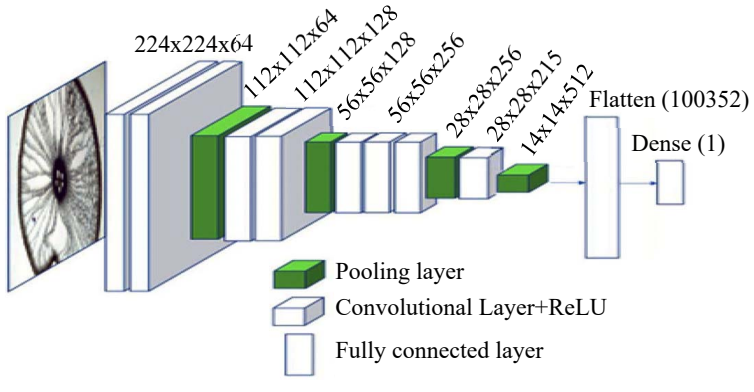

a

Model: "sequential_3"		
Layer (type)	Output shape	Param#
Conv2d_1 (Conv2D)	(None, 224, 224, 64)	1,792
Conv2d_2 (Conv2D)	(None, 224, 224, 64)	36,928
Maxpooling2d_1 (MaxPooling2D)	(None, 112, 112, 64)	0
Conv2d_3 (Conv2D)	(None, 112, 112, 128)	73,856
Conv2d_4 (Conv2D)	(None, 112, 112, 128)	147,584
Maxpooling2d_2 (MaxPooling2D)	(None, 56, 56, 128)	0
Conv2d_5 (Conv2D)	(None, 56, 56, 256)	295,168
Conv2d_6 (Conv2D)	(None, 56, 56, 256)	590,080
Conv2d_7 (Conv2D)	(None, 56, 56, 256)	590,080
Maxpooling2d_3 (MaxPooling2D)	(None, 56, 56, 256)	0
Conv2d_8 (Conv2D)	(None, 28, 28, 512)	1,180,160
Maxpooling2d_4 (MaxPooling2D)	(None, 14, 14, 512)	0
Flatten_1 (Flatten)	(None, 100352)	0
Dense_1 (Dense)	(None, 1)	100,353
Total params: 3,016,001 Trainable params: 3,016,001 Non-trainable params: 0		

b

Fig. 5. Details of a new deep network for the second proposed model: *a* – the proposed deep learning networks; *b* – variables summary of the proposed deep learning networks

It can be observed that these deep learning networks possess noteworthy characteristics, such as a limited number of layers, restricted variables, and quick response time, while still maintaining a high level of accuracy compared to similar deep learning networks used in the first architecture. The figure reveals that the number of network variables has decreased from 14,739,777 to 3,016,001, resulting in a network size that is approximately 4.8 times smaller than in the first model. Despite this reduction in size, the performance accuracy remains almost the same as in the first model. The small size of the deep learning network used as a classifier in the embedded model offers several advantages. Firstly, it offers faster performance due to the network comprising only a few layers. Secondly, the network requires only a small number of variables to build, which results in less storage space and memory handling, thereby increasing performance speed and reducing energy consumption. Additionally, the system structure's adoption of parallel architectures enables it to operate simultaneously, detecting and differentiating multiple diseases from one or multiple inputs simultaneously. The model's small size and high performance also make it less energy-intensive, making it ideal for self-powered systems and light IoT applications.

To enable our proposed model to be remote and standalone, without depending on any computer system or high-cost, high power consumption components, the Jetson Nano platform, model P3448-0000, shown in Fig. 6 has been chosen. The NVIDIA Jetson Nano Developer Kit is designed to provide makers, learners, and developers with a low-power and user-friendly platform to harness the power of modern artificial intelligence.

Fig. 6. The chosen development kit

With its pre-configured support for various popular peripherals, add-ons, and readily available projects, users can easily get started without delay [35]. Anyway, our Jetson Nano was configured through installing the operating system, TensorFlow with all the necessary libraries. After that, the proposed models were implemented in this kit. The development kit offers the advantage of being a multi-core processor, enabling support for the parallel architecture utilized in implementing the proposed models.

5. Results of multi-label embedded parallel models for ocular disease detection and classification

5. 1. Production accuracy of the Multi-label parallel embedded architecture transfer learning-based model

For cataract (C) detection vs. normal (N), we take the same number for both of Cataract class and Normal class, then we pass the data into pretraining VGG16 and get training accuracy and validation accuracy, as shown in Fig. 7.

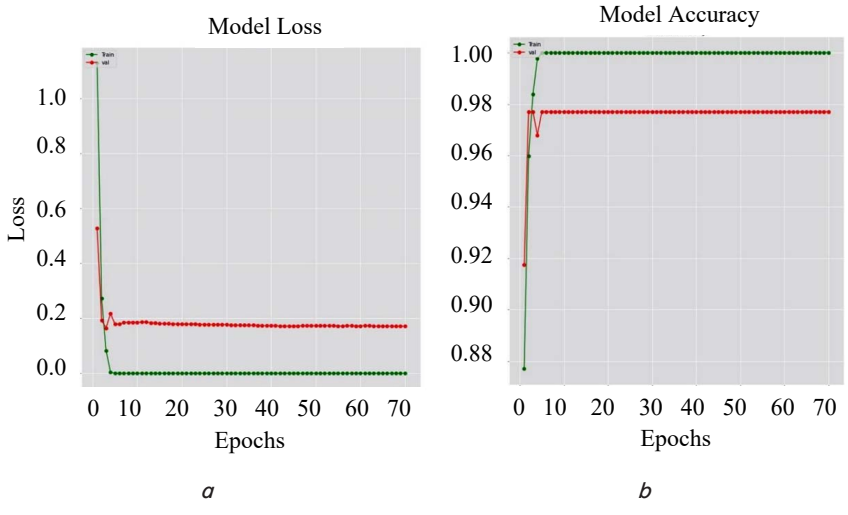

Fig. 7. Cataract detection: *a* – model accuracy; *b* – loss for N vs. C for VGG16; — train; — val

And after 70 epochs for VGG16, the training and validation accuracy for VGG16 was 1.0 and 0.977, respectively. For glaucoma (G) detection vs. normal (N), as in cataract, we extracted a sample of data from the dataset and used a pre-trained VGG16 model to compute the training accuracy and loss, and the results were as in Fig. 8.

As shown in Fig. 8, the training and validation accuracy for VGG16 was about 1.0, and 0.9487, respectively.

For hypertension (H) detection vs. normal (N), we collected data from the dataset and passed it into a pre-trained VGG16 to calculate training accuracy and loss as shown in Fig. 9.

As shown in Fig. 9, the training accuracy was 1.0, while the validation accuracy was 0.9096. For moderate non-proliferative retinopathy (D) detection vs. normal (N), we obtained the training accuracy and loss by extracting a sample of data from the ODIR dataset and inputting it into a VGG16 model. The resulting output is illustrated in Fig. 10.

As shown in Fig. 10, the training accuracy was about 1.0, while the validation accuracy was about 0.86027.

For age-related macular degeneration (A) vs. normal (N), like previously, we utilized a pre-trained VGG16 model to analyze the sample data for the current Ocular Disease and get both training accuracy, validation accuracy, and loss, as shown in Fig. 11.

So, as shown in Fig. 12, these values were 1.0, 0.8789, respectively.

For Myopia (M) detection vs. normal (N), we employed the identical approach as before by extracting data from inputting it into a pre-existing VGG16 model to compute the results.

So, the training accuracy, validation accuracy, and loss were 1.0, 0.9947, and 0.0214, respectively, after 70 epochs as shown in Fig. 12.

Finally, for Other Diseases/Abnormalities (O) detection vs. normal (N), the ODIR dataset comprises over eight distinct ocular diseases, while the remaining eye conditions were categorized as "other abnormal conditions". Similar to the ocular diseases, data for these conditions were extracted from the dataset and fed into a pre-existing VGG16 model for training and validation. The results after 70 epochs were 1.0, and 0.85 for both training and validation accuracy, while the loss was 1.3, as shown in Fig. 13.

Also, Fig. 14 displays the confusion matrix for each ocular disease compared to the normal state.

These confusion matrices offer comprehension of the evaluation metrics, including recall, precision, and accuracy, for the proposed model.

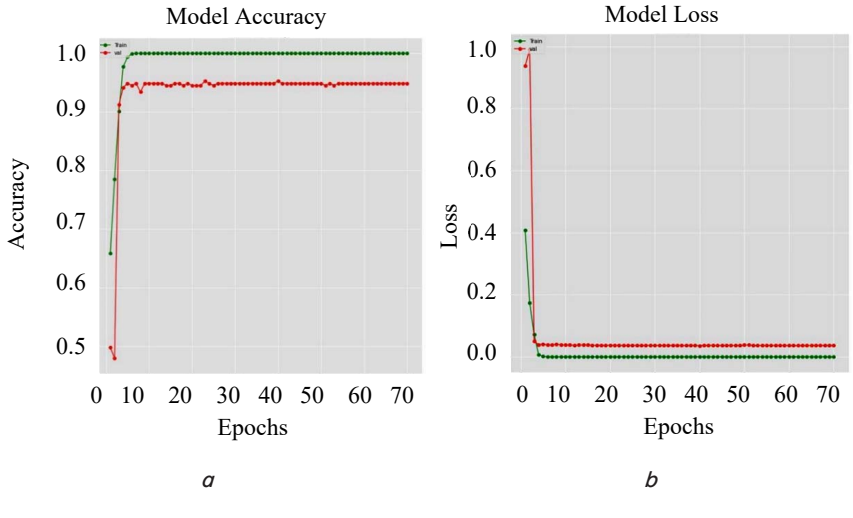

Fig. 8. Glaucoma detection: *a* – model accuracy; *b* – loss for N vs. G for VGG16; — train; — val

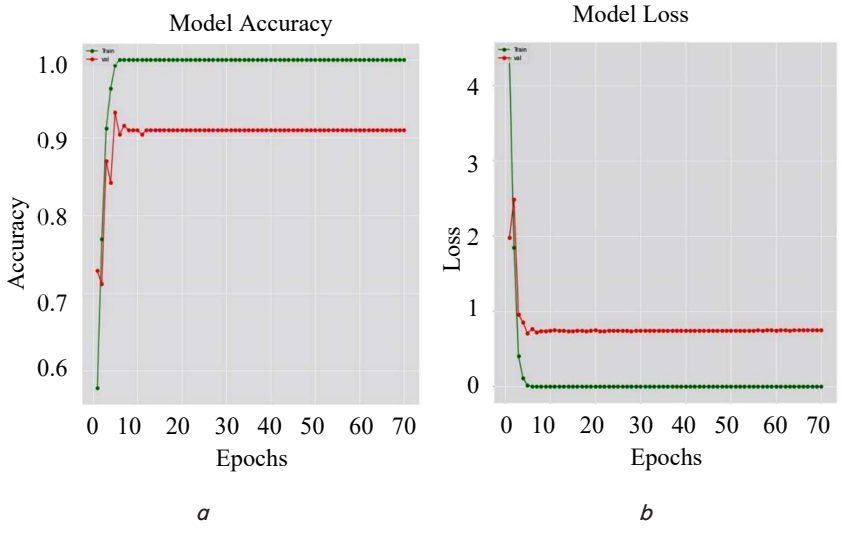

Fig. 9. Hypertension detection: *a* – model accuracy; *b* – loss for N vs. H; — train; — val

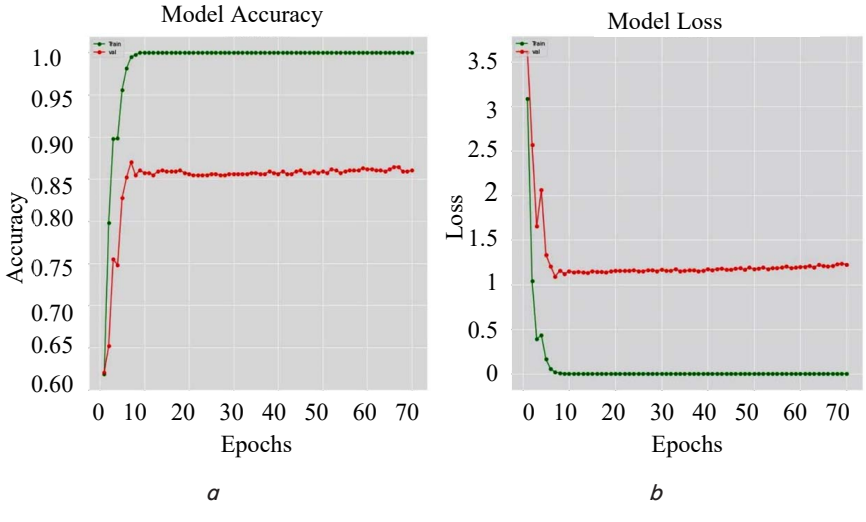

Fig. 10. Moderate non-proliferative retinopathy: *a* – model accuracy; *b* – loss for N vs. D; — train; — val

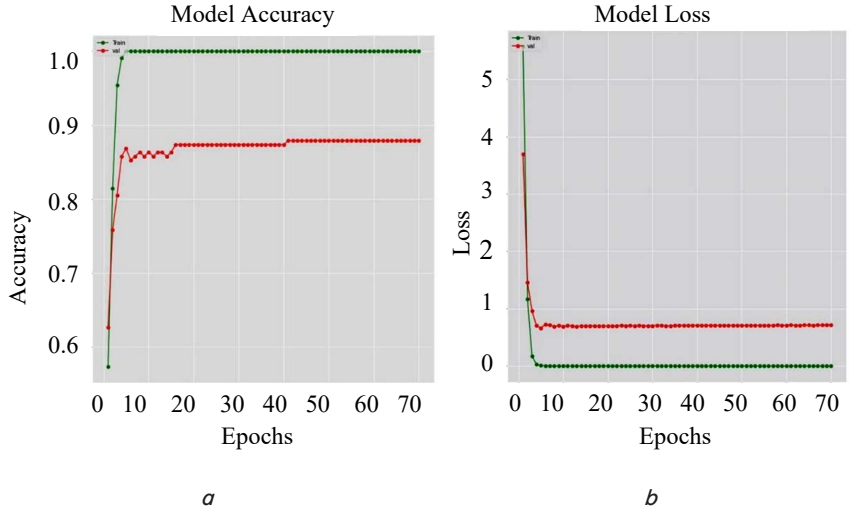

Fig. 11. Age-related macular degeneration detection:
a – model accuracy; *b* – loss for N vs. A; — train; — val

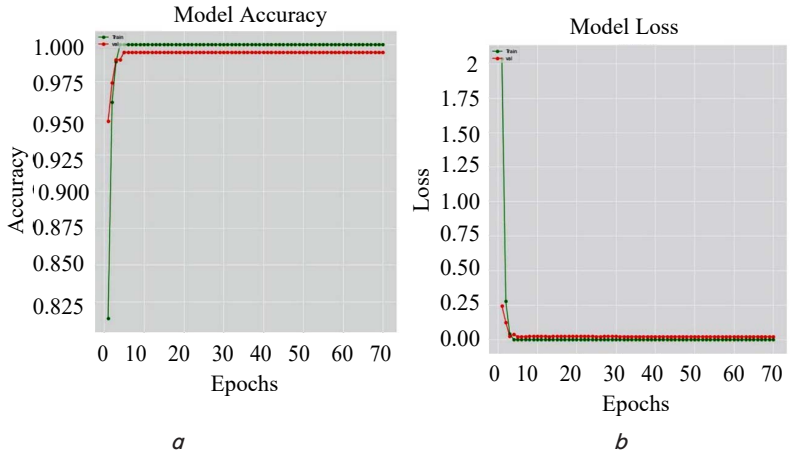

Fig. 12. Myopia detection: *a* – model accuracy; *b* – loss for N vs. M for VGG16; — train; — val

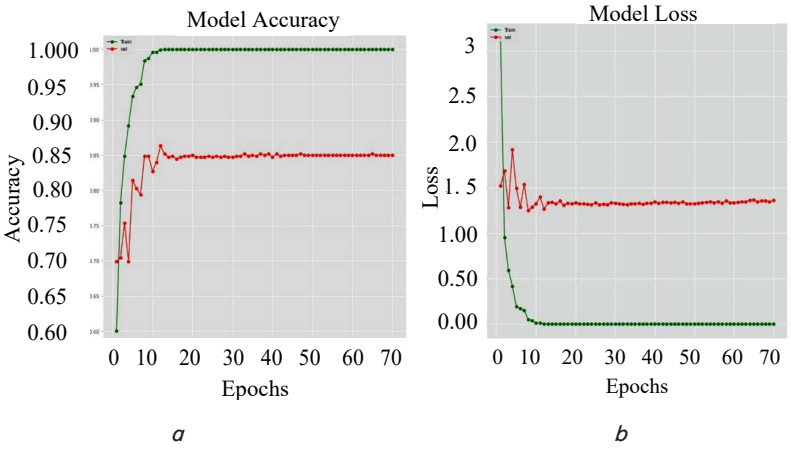

Fig. 13. Other ocular disease detection: *a* – model accuracy; b – loss for N vs. O; — train; — val

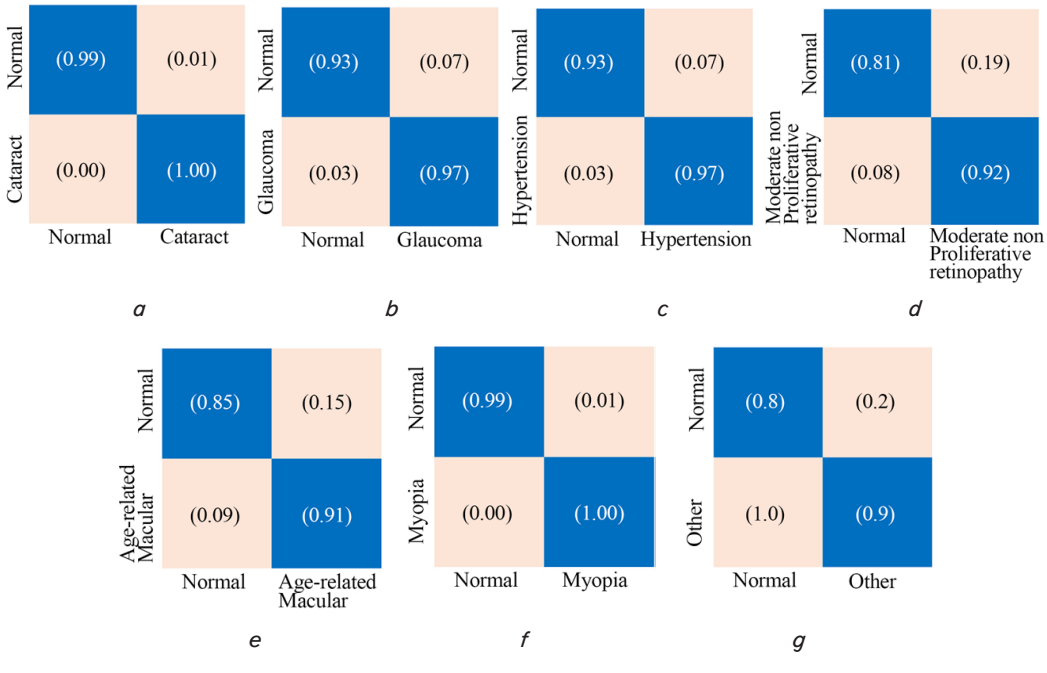

Fig. 14. Confusion matrix of the first proposed model: *a* – confusion matrix for N versus C classification; *b* – confusion matrix for N versus G classification, *c* – confusion matrix for N versus H classification; *d* – confusion matrix for N versus D classification; *e* – confusion matrix for N versus A classification; *f* – confusion matrix for N versus M classification; *g* – confusion matrix for N versus O classification

5. 2. Production accuracy of the Multi-label parallel embedded architecture novel deep network-based model

For cataract (C) detection vs. normal (N), we obtained the training accuracy, validation accuracy, and loss by extracting a sample of data from the ODIR dataset and inputting it into a new deep learning network as shown in Fig. 15.

As Fig. 15 shows, we got 0.9805 and 0.9403 for both training accuracy and validation accuracy.

For hypertensive retinopathy (H) detection vs. normal (N), again we calculated training accuracy, validation accuracy, and loss via sampled data from the dataset and fed them into our new deep learning network to get the results in Fig. 16.

So after 70 epochs, we got 0.9968 as training accuracy, while the validation accuracy was 0.8853.

For dry age-related macular (A) detection vs. normal (N), and in the same manner, we calculated training accuracy and validation accuracy via sampled data from the dataset and fed them into our compacted learning network. The results are shown in Fig. 17.

As shown in Fig. 17, the training accuracy was about 0.9939, while the validation accuracy was 0.9356.

Finally, for myopia (M) detection vs. normal (N), and after 70 epochs, the results are shown in Fig. 18.

We got about 0.9791 and 0.96 as training and validation accuracy, respectively.

However, during the training process of the model, we assess its ability to learn from the training data and improve its accuracy. The main goal of training precision is to identify any issues, such as overfitting or underfitting, and optimize hyperparameters accordingly. Once the model has been trained using the training dataset and validated using a separate validation dataset, we can determine its final accuracy by evaluating its performance on the test dataset. Accuracy is shown in (1):

$$\text{Accuracy} = \frac{\text{True Positive} + \text{True Negative}}{\text{True Positive} + \text{True Negative} + \text{False Positive} + \text{FalseNegative}}. \quad (1)$$

The accuracy achieved by each of the two models proposed in this research study is summarized in Table 1.

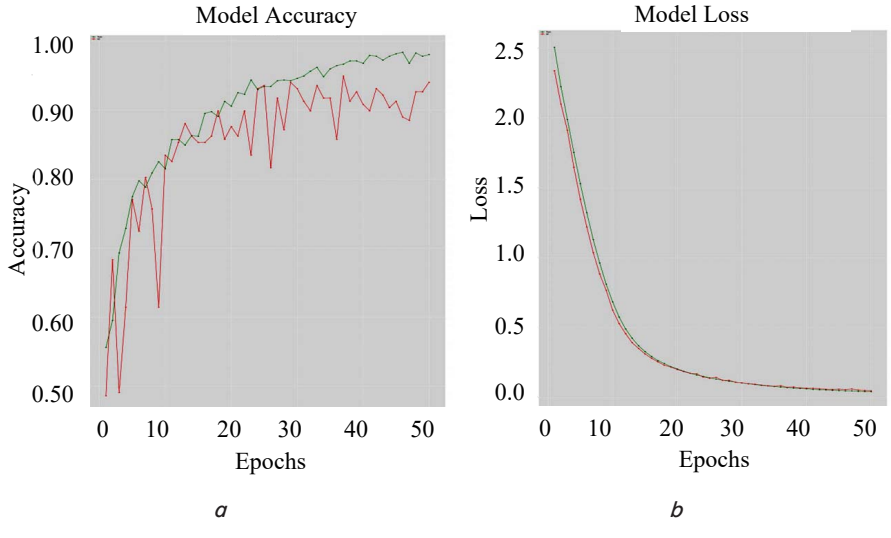

a *b*

Fig. 15. Cataract detection: *a* – model accuracy; *b* – loss for N vs. C for the compact network; — train; — val

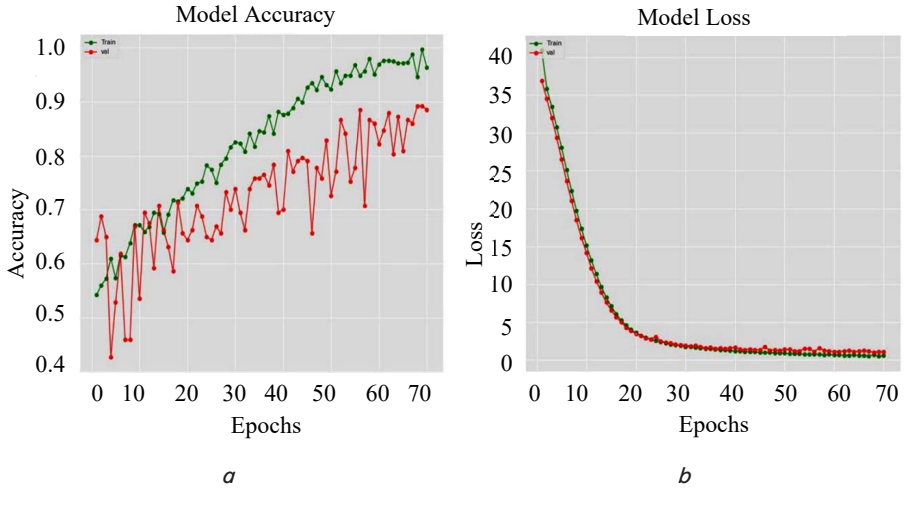

a *b*

Fig. 16. Hypertension detection: *a* – model accuracy; *b* – loss for N vs. H for the compact network; — train; — val

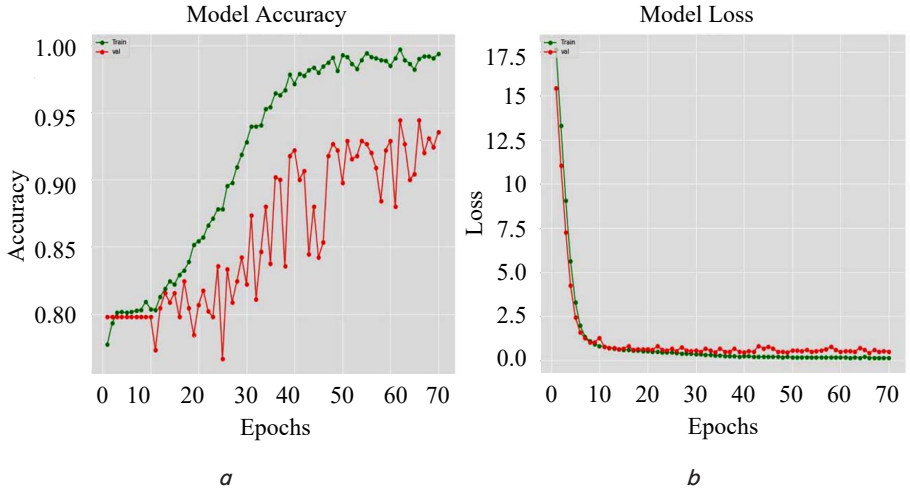

Fig. 17. Age-related macular degeneration detection: *a* – model accuracy; *b* – loss for N vs. A for the compact network; — train; — val

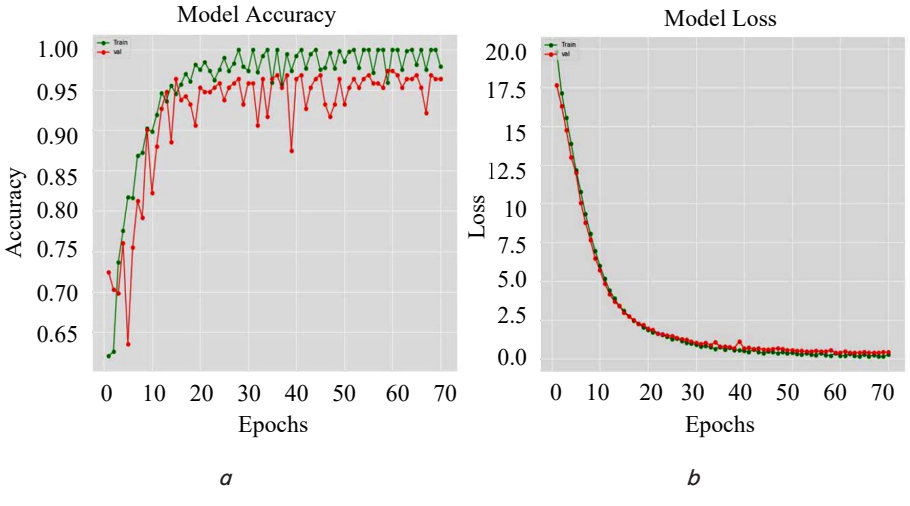

Fig. 18. Myopia detection: *a* – model accuracy; *b* – loss for N vs. M for the compact network; — train; — val

Table 1

Test accuracy results

Ocular Disease	Transfer Learning model	New deep Net. model
	Validation accuracy	Validation accuracy
Cataract	0.977	0.9403
Glaucoma	0.9487	0.905
Hypertension	0.9096	0.8853
Moderate non-proliferative retinopathy	0.86027	0.846
Age-related Macular Degeneration	0.8789	0.9356
Myopia	0.9947	0.96
Other	0.870	0.861

Occasionally, relying on the accuracy, shown in equation (1), is insufficient. To evaluate the efficacy of determining whether a particular image represents a disease, we incorporate various metrics related to accuracy. As we have employed classification models, we utilize the most prevalent metrics for classification problems, including Precision, Recall, and F1 Score. The amalgamation of these metrics with accurate measurement will provide a comprehensive overview of the quality of the classification system.

Precision provides a measure of the proportion of disease-positive patients correctly identified among the entire dataset. Precision is shown in (2):

$$\text{precision} = \frac{\text{True Positive}}{\text{True Positive} + \text{False Positive}}. \quad (2)$$

Recall assesses the number of true positives that have been accurately classified, which in our prediction models refers to individuals who are truly afflicted and have been predicted by our model to be afflicted. Recall is shown in (3):

$$\text{Recall} = \frac{\text{True Positive}}{\text{True Positive} + \text{False Negative}}. \quad (3)$$

F1 score is a common evaluation metric used in deep learning for binary classification tasks. It combines the precision and recall of a classifier into a single value, which evaluates the overall performance of a binary classifier. The F1 score ranges from 0 to 1, with a higher score

indicating better performance. The F1 score is calculated as in (4):

$$\text{F1 Score} = \frac{\text{Precision} * \text{Recall}}{\text{Precision} + \text{Recall}}. \quad (4)$$

So, Precision, Recall, and F1 Score, which are a comprehensive view of the proposed systems' performance, are shown in Fig. 19. The criteria mentioned are considered as a means of validation and confirmation of the results obtained by the two proposed models. Both 19-A and 19-B are divided into seven binary subgroups representing the metrics of the seven classifiers compared to the normal state. Each subgroup is denoted by Class 0 and Class 1, indicating the absence or presence of a specific eye disease. This figure presents the Precision, Recall, and F1 Score values for each class.

A comparison of our model's performance with other published studies for reference is conducted in Table 2. It provides an overview of the models utilized in each study, indicating the size of the corresponding Deep Learning Network. Additionally, it highlights the diagnostic accuracy achieved by each system after training on the ODIR dataset.

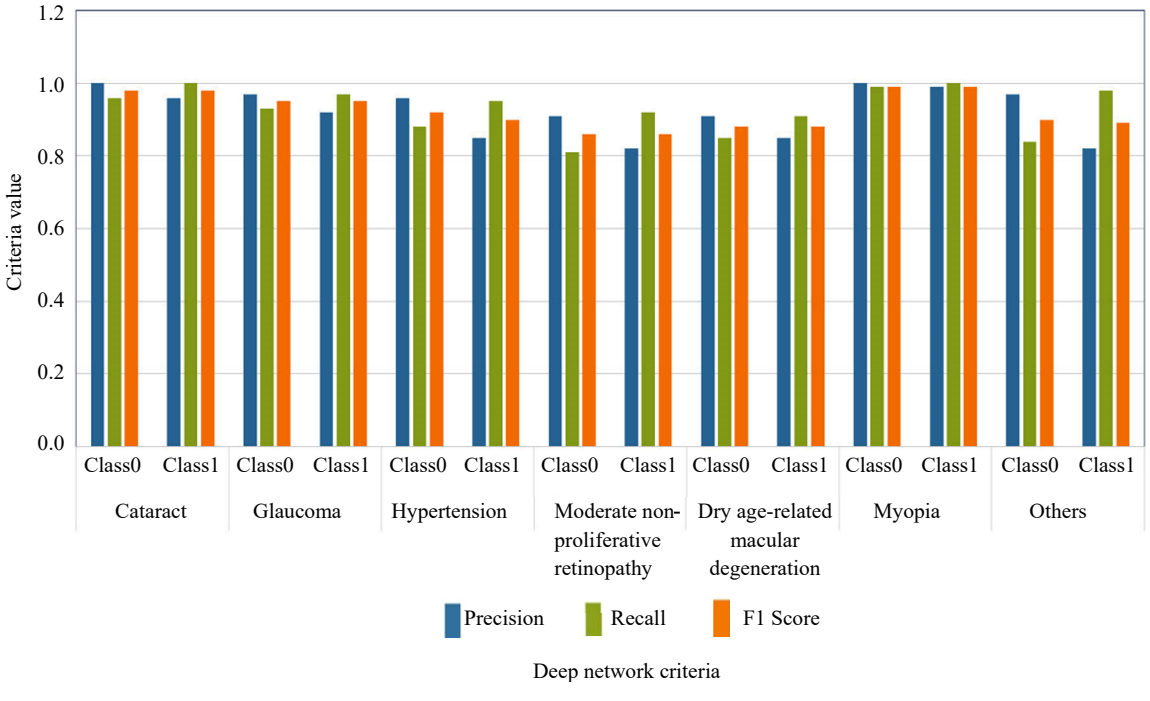

a

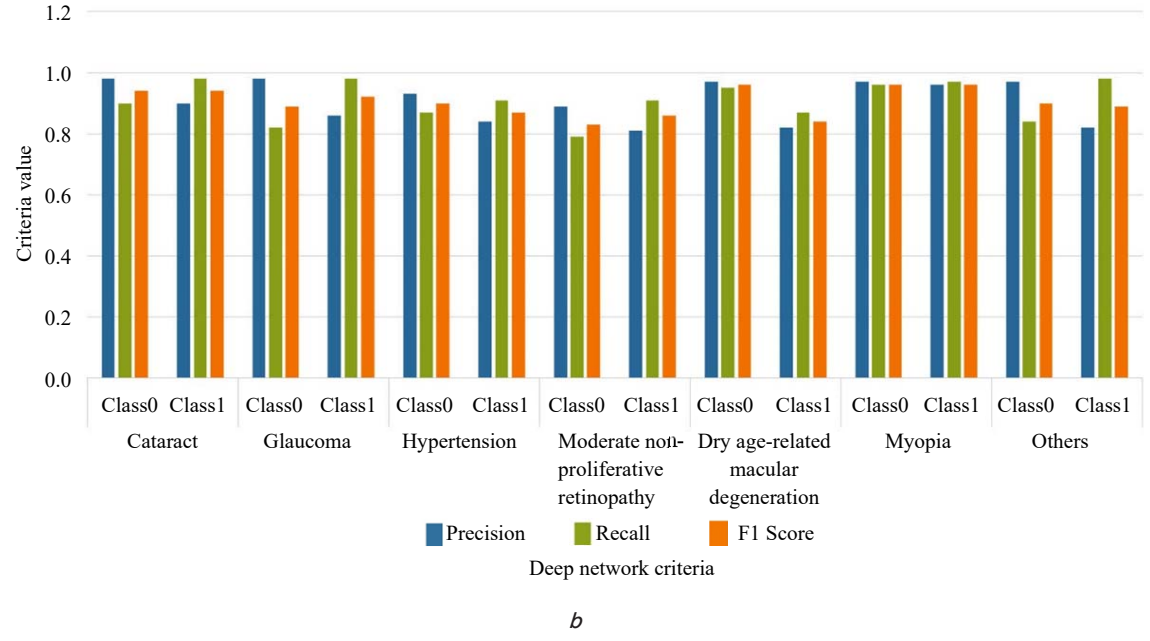

b

Fig. 19. Performance metrics of each class for multi-label parallel embedded architecture: *a* — transfer learning based; *b* — new deep Net. based

Table 2

Various techniques for comparison

Paper reference	Model	Model size (Total Training variables)	Accuracy	Our first model based on (Transfer learning)	Our second model based on (New deep Net.)
[36]	EFFICIENTNET B3	10,711,602	0.920	0.9947	0.96
[37]	RESNET-101	42,200,000	0.930		
[38]	MOBILE NETV2	34,112,000	0.9432		
[39]	VGG16	15,135,624	0.8906		
[40]	Sequential model of DENSENET201 AND EFFICIENTNETB4 AND RESNET105	87,515,476	0.9742		
[41]	RESNET-18	11,400,000	0.914		
	RESNET-34	21,500,000	0.924		
	RESNET-50	23,900,000	0.928		
[42]	EFFICIENTNET B7	66,000,000	0.8823		
[43]	Sequential model of INCEPTION RESNET AND DKC BLOCK	56,000,000	0.9608		
[44]	RESNET50	23,900,000	0.9710		
[45]	RESNEXT50	27,560,000	0.8606		

Upon closer examination of Table 2, it becomes evident that previous studies utilized various techniques to achieve satisfactory outcomes. Although some of these approaches were similar, their results varied, indicating that researchers in this domain have introduced enhancements and innovations. Nonetheless, Table 2 unequivocally demonstrates the superiority of the embedded models proposed in this investigation. The initial model exhibits a remarkable advantage in performance compared to its transfer learning-based counterparts. Moreover, the second proposed model exhibits a clear distinction in terms of efficiency and accuracy in performance, depending on the size of the small deep learning networks adopted for classification. This model competes with renowned deep learning networks such as VGG16, EfficientNetB3, and RESNET50.

The disparity in size between the deep learning networks employed in prior studies and those proposed in the second model is illustrated clearly in Fig. 20.

As shown in Fig. 20, a marked difference can be observed in the size of the deep learning network proposed for the second model in this study, compared to other deep learning networks. However, the classification performance and accuracy of this network are representatives of those networks, and are sometimes agreed upon.

6. Discussion of experimental results of the proposed Multi-label parallel embedded models for ocular disease detection and classification

The incorporation of parallel architectures in the implementation of the deep learning system as shown in (Fig. 3), instead of relying on a single deep network, proved highly advantageous in each of the proposed development models, where this methodology converts the computation complexity of the deep networks, to set of parallel more easiest computation deals with a binary classifier only. Also, parallelism gives complete flexibility when dealing with system inputs, wherein the proposed models can diagnose multiple diseases for various inputs simultaneously. Furthermore, it can diagnose several ailments for a specific condition simultaneously.

Additionally, the new implementation plays a crucial role in improving accuracy, precision, recall, and F1 score, as demonstrated in Table 1 and Fig. 19, which provides multiple and comprehensive criteria that confirm the superiority of the proposed models and the accuracy of their performance. This explains the superior performance of the proposed models compared to their counterparts, namely [36–38], which have been conducted in a similar scholarly research field.

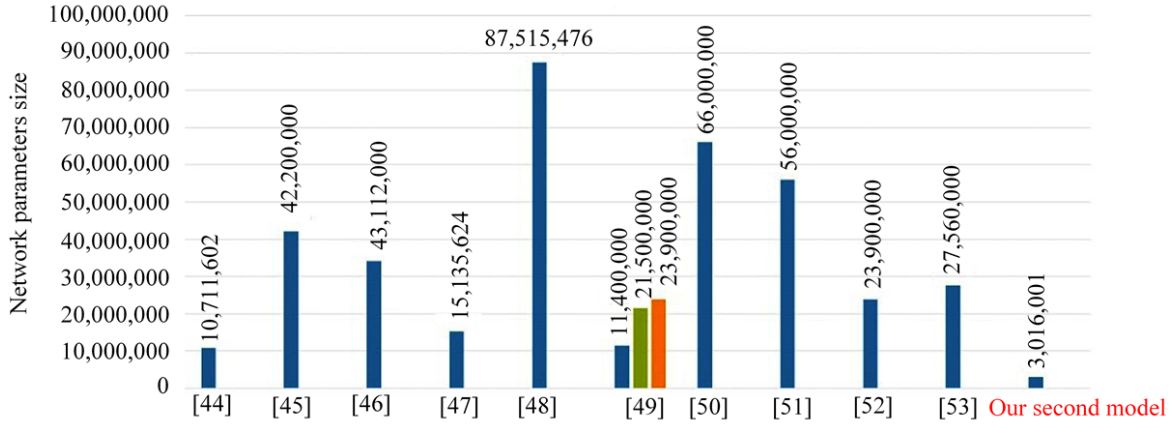

Fig. 20. Models size comparison based on network parameters

Table 2 highlights the notable improvement in diagnostic accuracy provided by the two suggested models compared to the aforementioned studies.

Besides that, the adoption of new deep learning networks in the implementation of the proposed model also added to a clear reduction in the classifier size of the deep learning systems that are presented in [40, 42, 43, 45]. Fig. 20 illustrates the decrease in the suggested deep networks' size compared to the networks utilized in those studies. Where the reduction percentages are 29 %, 21 %, 18.56 %, and 9.13 % for each of the works, respectively. Consequently, the proposed model of such deep networks has played a significant role in reducing resource consumption. Furthermore, it has enabled the utilization of such networks on affordable hardware resources, like Jetson Nano, and Raspberry Pi, that have limited energy consumption capabilities.

Hence, the functioning of the proposed embedded systems extends beyond the realm of eye disease diagnosis and classification. These systems can be effectively utilized in various artificial intelligence applications related to image detection and classification with a simple modification, and by training the networks of these systems with suitable databases, their potential can be harnessed across diverse domains in this field.

The most important limitation and challenge of this study is that it contains a collection of low-quality images. Despite the preprocessing and diversity of the database regarding the people race groups, the number of pathological cases it contains, the inclusion of fundus images for each of the patient's eyes, and the variety of sources used to provide fundus images, however, it includes blurry, dark, and unclear images that negatively impacted the obtained results. One possible proposed solution for addressing this issue is to use deep learning for further comprehension preprocessing to smooth images and highlight the most valuable features in the database.

Another developed research work can be through the employment of SIMD architecture as a means to implement deep networks, which can be utilized to construct classification models. This is due to its rapid execution of parallel commands, thereby reducing execution time.

Meanwhile, it is advantageous to consider the proposed approaches to improve power efficiency by utilizing the embedded systems described in this research on FPGA platforms, where these platforms are recognized for their exceptional energy efficiency.

7. Conclusions

1. Eight eye diseases were diagnosed simultaneously through a parallel architecture embedded in two proposed models of deep learning systems, where the accuracy of performance was about 0.9947 and 0.96 for both proposed models, respectively. Also, the response speed of both proposed systems was very high due to the adoption of parallelism in the implementation of the deep network instead of the previously adopted consecutive, where the performance speed of the presented models was 25.8119 ms and 3.0121 ms, respectively, when both models were tested on a PC of Intel® Core™ i9-9900K CPU @ 3.60GHz 3.60 GHz, 32GB RAM, and 64-bit Operating System before implementing them as an embedded system on the developer kit.

2. The proposed new deep learning networks with limited layers and variables significantly contributed to reducing the resource and capacity requirements of the proposed systems compared to other deep learning networks. Where the total number of the proposed network variables reached only 3,016,001 while maintaining efficiency and accuracy of performance.

The architectures presented in this study can be invested in IoT applications supporting deep learning, as well as the possibility of using them in smart applications for remote-operated systems and self-powered models.

Conflict of interest

The authors declare that they have no conflict of interest in relation to this research, whether financial, personal, authorship or otherwise, that could affect the research and its results presented in this paper.

Financing

The study was performed without financial support.

Data availability

The manuscript has associated data in a data repository.

Acknowledgments

The researchers would like to extend their thanks and appreciation to Ninevah University/College of Electronics Engineering/Computer and Information Engineering department, and Mosul/College of Engineering/Computer Engineering department for their support, which has assisted to boost the outcomes of this research paper.

References

1. Alwakid, G., Gouda, W., Humayun, M. (2023). Deep Learning-Based Prediction of Diabetic Retinopathy Using CLAHE and ESRGAN for Enhancement. Healthcare, 11 (6), 863. doi: https://doi.org/10.3390/healthcare11060863
2. Marouf, A. A., Mottalib, M. M., Alhajj, R., Rokne, J., Jafarullah, O. (2022). An Efficient Approach to Predict Eye Diseases from Symptoms Using Machine Learning and Ranker-Based Feature Selection Methods. Bioengineering, 10 (1), 25. doi: https://doi.org/10.3390/bioengineering10010025
3. Albahli, S., Ahmad Hassan Yar, G. N. (2022). Automated detection of diabetic retinopathy using custom convolutional neural network. Journal of X-Ray Science and Technology, 30 (2), 275–291. doi: https://doi.org/10.3233/xst-211073
4. Ebri, A. E., Govender, P., Naidoo, K. S. (2019). Prevalence of vision impairment and refractive error in school learners in Calabar, Nigeria. African Vision and Eye Health, 78 (1). doi: https://doi.org/10.4102/aveh.v78i1.487

5. Pakbin, M., Katibeh, M., Pakravan, M., Yaseri, M., Soleimanizad, R. (2015). Prevalence and causes of visual impairment and blindness in central Iran; The Yazd eye study. Journal of Ophthalmic and Vision Research, 10 (3), 279. doi: https://doi.org/10.4103/2008-322x.170362
6. Elzean, C., Sakr, E. (2021). Proposed three-dimensional designs for the color wheel to help blind persons understand matching colors of their clothes. International Design Journal, 11 (2), 417–423. doi: https://doi.org/10.21608/idj.2021.153624
7. Demir, F., Taşcı, B. (2021). An Effective and Robust Approach Based on R-CNN+LSTM Model and NCAR Feature Selection for Ophthalmological Disease Detection from Fundus Images. Journal of Personalized Medicine, 11 (12), 1276. doi: https://doi.org/10.3390/jpm11121276
8. Biswas, R. K., Rahman, N., Islam, H., Senserrick, T., Bhowmik, J. (2020). Exposure of mobile phones and mass media in maternal health services use in developing nations: evidence from Urban Health Survey 2013 of Bangladesh. Contemporary South Asia, 29 (3), 460–473. doi: https://doi.org/10.1080/09584935.2020.1770698
9. Alam, K. N., Khan, M. S., Dhruba, A. R., Khan, M. M., Al-Amri, J. F., Masud, M., Rawashdeh, M. (2021). Deep Learning-Based Sentiment Analysis of COVID-19 Vaccination Responses from Twitter Data. Computational and Mathematical Methods in Medicine, 2021, 1–15. doi: https://doi.org/10.1155/2021/4321131
10. He, J., Li, C., Ye, J., Qiao, Y., Gu, L. (2021). Self-speculation of clinical features based on knowledge distillation for accurate ocular disease classification. Biomedical Signal Processing and Control, 67, 102491. doi: https://doi.org/10.1016/j.bspc.2021.102491
11. Kadhim, Y. A., Khan, M. U., Mishra, A. (2022). Deep Learning-Based Computer-Aided Diagnosis (CAD): Applications for Medical Image Datasets. Sensors, 22 (22), 8999. doi: https://doi.org/10.3390/s22228999
12. Roy, A. G., Conjeti, S., Karri, S. P. K., Sheet, D., Katouzian, A., Wachinger, C., Navab, N. (2017). ReLayNet: retinal layer and fluid segmentation of macular optical coherence tomography using fully convolutional networks. Biomedical Optics Express, 8 (8), 3627. doi: https://doi.org/10.1364/boe.8.003627
13. Lee, C. S., Tyring, A. J., Deruyter, N. P., Wu, Y., Rokem, A., Lee, A. Y. (2017). Deep-learning based, automated segmentation of macular edema in optical coherence tomography. Biomedical Optics Express, 8 (7), 3440. doi: https://doi.org/10.1364/boe.8.003440
14. Oda, M., Yamaguchi, T., Fukuoka, H., Ueno, Y., Mori, K. (2020). Automated eye disease classification method from anterior eye image using anatomical structure focused image classification technique. Medical Imaging 2020: Computer-Aided Diagnosis. doi: https://doi.org/10.1117/12.2549951
15. Maaliw, R. R., Alon, A. S., Lagman, A. C., Garcia, M. B., Abante, M. V., Belleza, R. C. et al. (2022). Cataract Detection and Grading Using Ensemble Neural Networks and Transfer Learning. 2022 IEEE 13th Annual Information Technology, Electronics and Mobile Communication Conference (IEMCON). doi: https://doi.org/10.1109/iemcon56893.2022.9946550
16. Marrapu, H. K. (2022). Detection of Glaucoma Using Deep Learning Techniques: Literature Survey. Specialusis Ugdymas, 1 (43), 8089–8098. URL: http://www.sumc.lt/index.php/se/article/view/1182/915
17. Kashyap, R., Nair, R., Gangadharan, S. M. P., Botto-Tobar, M., Farooq, S., Rizwan, A. (2022). Glaucoma Detection and Classification Using Improved U-Net Deep Learning Model. Healthcare, 10 (12), 2497. doi: https://doi.org/10.3390/healthcare10122497
18. Bhimavarapu, U., Battineni, G. (2022). Deep Learning for the Detection and Classification of Diabetic Retinopathy with an Improved Activation Function. Healthcare, 11 (1), 97. doi: https://doi.org/10.3390/healthcare11010097
19. Fan, R., Bowd, C., Christopher, M., Brye, N., Proudfoot, J. A., Rezapour, J. et al. (2022). Detecting Glaucoma in the Ocular Hypertension Study Using Deep Learning. JAMA Ophthalmology, 140 (4), 383. doi: https://doi.org/10.1001/jamaophthalmol.2022.0244
20. Lin, M., Hou, B., Liu, L., Gordon, M., Kass, M., Wang, F. et al. (2022). Automated diagnosing primary open-angle glaucoma from fundus image by simulating human's grading with deep learning. Scientific Reports, 12 (1). doi: https://doi.org/10.1038/s41598-022-17753-4
21. Santos-Bustos, D. F., Nguyen, B. M., Espitia, H. E. (2022). Towards automated eye cancer classification via VGG and ResNet networks using transfer learning. Engineering Science and Technology, an International Journal, 35, 101214. doi: https://doi.org/10.1016/j.jestch.2022.101214
22. Abdelmotaal, H., Hazarbasanov, R., Taneri, S., Al-Timemy, A., Lavric, A., Takahashi, H., Yousefi, S. (2023). Detecting dry eye from ocular surface videos based on deep learning. The Ocular Surface, 28, 90–98. doi: https://doi.org/10.1016/j.jtos.2023.01.005
23. Choudhary, A., Ahlawat, S., Urooj, S., Pathak, N., Lay-Ekuakille, A., Sharma, N. (2023). A Deep Learning-Based Framework for Retinal Disease Classification. Healthcare, 11 (2), 212. doi: https://doi.org/10.3390/healthcare11020212
24. Park, S.-J., Ko, T., Park, C.-K., Kim, Y.-C., Choi, I.-Y. (2022). Deep Learning Model Based on 3D Optical Coherence Tomography Images for the Automated Detection of Pathologic Myopia. Diagnostics, 12 (3), 742. doi: https://doi.org/10.3390/diagnostics12030742
25. Seif, G. (2018). Handling imbalanced datasets in deep learning. URL: https://towardsdatascience.com/handling-imbalanced-datasets-in-deep-learning-f48407a0e758
26. Hodge, W. G., Whitcher, J. P., Satariano, W. (1995). Risk Factors for Age-related Cataracts. Epidemiologic Reviews, 17 (2), 336–346. doi: https://doi.org/10.1093/oxfordjournals.epirev.a036197
27. Liu, Y.-C., Wilkins, M., Kim, T., Malyugin, B., Mehta, J. S. (2017). Cataracts. The Lancet, 390 (10094), 600–612. doi: https://doi.org/10.1016/s0140-6736(17)30544-5
28. Al-Jarrah, M. A., Shatnawi, H. (2017). Non-proliferative diabetic retinopathy symptoms detection and classification using neural network. Journal of Medical Engineering & Technology, 41 (6), 498–505. doi: https://doi.org/10.1080/03091902.2017.1358772

29. Verkicharla, P. K., Ohno-Matsui, K., Saw, S. M. (2015). Current and predicted demographics of high myopia and an update of its associated pathological changes. Ophthalmic and Physiological Optics, 35 (5), 465–475. doi: https://doi.org/10.1111/opo.12238
30. Garcia-Villanueva, C., Milla, E., Bolarin, J. M., García-Medina, J. J., Cruz-Espinosa, J., Benítez-del-Castillo, J. et al. (2022). Impact of Systemic Comorbidities on Ocular Hypertension and Open-Angle Glaucoma, in a Population from Spain and Portugal. Journal of Clinical Medicine, 11 (19), 5649. doi: https://doi.org/10.3390/jcm11195649
31. Rakhmetulayeva, S., Syrymbet, Z. (2022). Implementation of convolutional neural network for predicting glaucoma from fundus images. Eastern-European Journal of Enterprise Technologies, 6 (2 (120)), 70–77. doi: https://doi.org/10.15587/1729-4061.2022.269229
32. Esengönül, M., Cunha, A. (2023). Glaucoma Detection using Convolutional Neural Networks for Mobile Use. Procedia Computer Science, 219, 1153–1160. doi: https://doi.org/10.1016/j.procs.2023.01.396
33. He, T., Zhou, Q., Zou, Y. (2022). Automatic Detection of Age-Related Macular Degeneration Based on Deep Learning and Local Outlier Factor Algorithm. Diagnostics, 12 (2), 532. doi: https://doi.org/10.3390/diagnostics12020532
34. Fang, H., Li, F., Fu, H., Sun, X., Cao, X., Lin, F. et al. (2022). ADAM Challenge: Detecting Age-Related Macular Degeneration From Fundus Images. IEEE Transactions on Medical Imaging, 41 (10), 2828–2847. doi: https://doi.org/10.1109/tmi.2022.3172773
35. Salih, T. A., Basman Gh., M. (2020). A novel Face Recognition System based on Jetson Nano developer kit. IOP Conference Series: Materials Science and Engineering, 928 (3), 032051. doi: https://doi.org/10.1088/1757-899x/928/3/032051
36. Wang, J., Yang, L., Huo, Z., He, W., Luo, J. (2020). Multi-Label Classification of Fundus Images With EfficientNet. IEEE Access, 8, 212499–212508. doi: https://doi.org/10.1109/access.2020.3040275
37. Li, C., Ye, J., He, J., Wang, S., Qiao, Y., Gu, L. (2020). Dense Correlation Network for Automated Multi-Label Ocular Disease Detection with Paired Color Fundus Photographs. 2020 IEEE 17th International Symposium on Biomedical Imaging (ISBI). doi: https://doi.org/10.1109/isbi45749.2020.9098340
38. Dipu, N. M., Alam Shohan, S., Salam, K. M. A. (2021). Ocular Disease Detection Using Advanced Neural Network Based Classification Algorithms. ASIAN JOURNAL OF CONVERGENCE IN TECHNOLOGY, 7 (2), 91–99. doi: https://doi.org/10.33130/ajct.2021v07i02.019
39. Gour, N., Khanna, P. (2021). Multi-class multi-label ophthalmological disease detection using transfer learning based convolutional neural network. Biomedical Signal Processing and Control, 66, 102329. doi: https://doi.org/10.1016/j.bspc.2020.102329
40. Kumar, E. S., Bindu, C. S. (2021). MDCF: Multi-Disease Classification Framework On Fundus Image Using Ensemble Cnn Models. Journal of Jilin University, 40 (09), 35–45. doi: https://doi.org/10.17605/OSF.IO/ZHA9C
41. He, J., Li, C., Ye, J., Qiao, Y., Gu, L. (2021). Multi-label ocular disease classification with a dense correlation deep neural network. Biomedical Signal Processing and Control, 63, 102167. doi: https://doi.org/10.1016/j.bspc.2020.102167
42. Boyina, L., Boddu, K., Tankasala, Y., Vani, K. S. (2022). Classification of Uncertain ImageNet Retinal Diseases using ResNet Model. International Journal of Intelligent Systems and Applications in Engineering, 10 (2s), 35–42. URL: https://ijisae.org/index.php/IJISAE/article/view/2358
43. Bhati, A., Gour, N., Khanna, P., Ojha, A. (2023). Discriminative kernel convolution network for multi-label ophthalmic disease detection on imbalanced fundus image dataset. Computers in Biology and Medicine, 153, 106519. doi: https://doi.org/10.1016/j.compbiomed.2022.106519
44. Emir, B., Colak, E. (2023). Performance analysis of pretrained convolutional neural network models for ophthalmological disease classification (Version 1). SciELO journals. doi: https://doi.org/10.6084/m9.figshare.22548323.v1
45. Mayya, V., S, S. K., Kulkarni, U., Surya, D. K., Acharya, U. R. (2022). An empirical study of preprocessing techniques with convolutional neural networks for accurate detection of chronic ocular diseases using fundus images. Applied Intelligence, 53 (2), 1548–1566. doi: https://doi.org/10.1007/s10489-022-03490-8